Communications in Physics, Vol. 36, No. 1 (2026), pp. 91-101
DOI: https://doi.org/10.15625/0868-3166/22927

Design and experimental evaluation of TiO_2/MgF_2 dual-layer anti-reflection coatings for Nd- and Er-doped phosphate glass lasers

Le Van Dai, **Do Thanh Tung**†, **Pham Duc Tuan and Truong Hong Giang**

Academy of Military Science and Technology, Nghia Do, Hanoi, Vietnam

E-mail: †tungitmo@gmail.com

Received 29 May 2025
Accepted for publication 19 November 2025
Published 5 March 2026

Abstract. *This study focuses on the design and experimental evaluation of two-layer TiO_2-MgF_2 anti-reflection (AR) coatings on Nd- and Er-doped phosphate glass for laser applications at 1053 nm and 1535 nm. Using matrix theory and TFCalc software, the optimized design achieves reflectance close to 0% for Nd-doped glass and below 0.1% for Er-doped glass. The coatings were fabricated using the SYRUSpro 710 system, achieving experimental transmittance values of 99.7% in the 1050–1080 nm range and 99.8% in the 1530–1570 nm range, despite minor discrepancies between experimental and simulated results. The coating durability meets MIL-SPEC standards for mechanical testing.Additionally, laser-induced damage threshold (LIDT) measurements at 1064 nm yielded a 50% damage fluence of 13.2 J/cm^2 for the Nd-doped sample, demonstrating reliable laser resistance suitable for moderate-fluence solid-state laser applications. This research lays the foundation for optimizing coating processes and advancing the development of rare-earth-doped solid-state laser sources.*

Keywords: anti-reflection; AR coating; Nd-doped; Er-doped; laser.
Classification numbers: 42.79.Wc; 78.20.Ci; 68.55.-a.

1. Introduction

Nd- and Er-doped phosphate glass lasers are critical sources of solid-state laser radiation in high-tech applications [1–6]. These lasers operate at eye-safe wavelengths and exhibit excellent amplification properties. Specifically, Nd-doped phosphate glass lasers emit radiation at 1053 nm, while Er-doped phosphate glass lasers operate at 1535 nm, making both suitable for high-precision systems such as range finders and optical communication [2, 5]. The core component of these lasers is the active medium, a phosphate glass rod doped with Nd_3^+ or Er_3^+ ions, which

facilitates stimulated emission when pumped by sources like flash lamps or laser diodes [2, 5]. However, a common issue in optical resonators is internal reflection at the surface of the active medium, which causes parasitic oscillations. This leads to unwanted light modes competing with the primary mode, significantly reducing the laser's efficiency and beam quality [7, 8]. To address this, anti-reflection (AR) coatings are applied to the surface of the active medium to minimize reflections and enhance amplification efficiency [9].

Designing an ideal AR coating for rare-earth-doped phosphate glass lasers is not a straightforward task, as it requires balancing optical performance, manufacturability, and durability in harsh operating environments [10, 11]. For a single-layer coating, theoretical conditions demand that the refractive index of the coating material equals the square root of the substrate's refractive index (the active medium) [12], approximately 1.24 for phosphate glass with a refractive index ranging from 1.53 to 1.535. However, transparent materials with such low refractive indices are rarely available in practice, making single-layer solutions impractical with conventional fabrication techniques. To overcome this, researchers have shifted toward multilayer systems, particularly two- or three-layer designs, which are easier to fabricate, mechanically robust, and stable over time compared to nanoporous or porous films with low effective refractive indices [13]. However, as the number of layers increases, the risk of laser-induced damage (LID) at the interfaces between layers also rises, necessitating a minimal number of layers to ensure reliability in high-power laser applications [12]. Previous studies have proposed various AR coating designs for Nd- and Er-doped lasers using common materials such as TiO_2, Al_2O_3, SiO_2, and MgF_2 [13–15]. For example, A. H. Jareeze designed antireflection coatings on glass substrates in single-, double-, and triple-layer configurations. In particular, by combining MgF_2 with CeF_3, the reflectance was reduced to about 0.5% at the wavelength of 1064 nm [13]. While V. H. Mai et al. designed a two-layer Al_2O_3-MgF_2 coating for Er-doped glass, achieving reflectance below 0.01% in the 1.53–1.57 μm range [14]. Nevertheless, combining theoretical calculations with experimental validation to assess the coating's effectiveness under real-world conditions remains insufficient.

The aim of this paper is to design and fabricate a two-layer anti-reflection coating for Nd-doped glass and Er-doped glass using TFCalc optimization and the SYRUSpro 710 coating system. The fabricated coating is required to meet the optical performance target of achieving a reflectance below 0.2% –a commonly referenced standard in laser optics [14] and to pass the laser-induced damage threshold (LIDT) test to confirm its applicability. The experimental results are then compared with simulation predictions to assess their suitability and practical applicability. The approach integrates matrix theory with TFCalc coating design software to optimize parameters such as the refractive index and thickness of each layer, utilizing TiO_2 and MgF_2 materials. The experimental coating process provides deeper insights into the discrepancies between theory and practice, enabling necessary adjustments to achieve optimal performance. This research contributes to improving the efficiency of Nd- and Er-doped lasers and lays the groundwork for developing AR coating fabrication processes, leveraging feasible techniques such as thermal evaporation and electron beam evaporation.

2. Materials and method

Nd- and Er-doped phosphate-glass substrates (supplied by SIOM [16]) were used for both simulations and experiments. Their nominal refractive indices were 1.535 ± 0.003 at 1053 nm (Nd-doped) and 1.530 ± 0.003 at 1535 nm (Er-doped), as summarized in Table 1. Each substrate

sample had dimensions of $12 \times 12 \times 2$ mm. Prior to coating, the substrates were pre-processed to meet laser-grade specifications: parallelism ≤ 15 arcsec, surface flatness $\geq \lambda/6$ at 632 nm, surface roughness $R_a \leq 1.5$ nm, surface quality 10-5 scratch-dig (MIL-PRF-13830B), and a clear aperture $\geq 90\%$ of the optical surface. These parameters were consistently applied in both the theoretical calculations and the experimental coating procedures described below.

Table 1. Optical parameters of Nd- and Er-doped glass.

Wavelength, λ [nm]	Nd-doped glass	Er-doped glass
Operating wavelength	1053	1535
Refractive index at wavelength	1.535 ± 0.003	1.530 ± 0.003

2.1. Theoretical design and calculations

The slight difference in the refractive indices of Nd- and Er-doped glass arises from the concentration of doped ions and the glass lattice structure. The refractive index of the substrate directly influences the conditions for reducing reflection at the air-active medium interface, as described in [17]:

$$R_S = R_I + \frac{R_I \cdot {T_I}^2 \exp(-2\alpha d)}{1 - {R_I}^2 \exp(-2\alpha d)} \tag{1}$$

with $R_I = \dfrac{(n-1)^2 + k^2}{(n+1)^2 + k^2}$, $T_I = 1 - R_I$ and $\alpha = (4\pi k)/\lambda$.

Here R_s is the reflectance of the substrate, R_I, and T_I are the reflectance and transmittance at the air-substrate interface, d is the substrate thickness, n and k are the real part and extinction coefficient of the substrate's complex refractive index, respectively.

AR coatings are typically designed with one or more homogeneous layers, characterized by a matrix M_j (where j is the number of layers), which depends on the refractive index n_j, the coating layer thickness d_j, and the wavelength λ [12, 18, 19]:

$$M_j = \begin{bmatrix} \cos\ \partial_j & \dfrac{i \sin \partial_j}{n_j} \\ i\, n_j \sin \partial_j & \cos \partial_j \end{bmatrix}, \tag{2}$$

where $\partial_j = \dfrac{2\pi n_j d_j}{\lambda}$ is the optical phase of the j-th layer, and i is the imaginary unit.

For a system with j layers, the total matrix M is the product of the individual matrices: $M = M_1 \cdot M_2 \cdot \ldots \cdot M_j$. The reflectance R of the entire system is calculated from the components of the total matrix M:

$$R = \left| \frac{n_0(M_{11} + M_{12} n_S) - (M_{21} + M_{22} n_S)}{n_0(M_{11} + M_{12} n_S) + (M_{21} + M_{22} n_S)} \right|^2. \tag{3}$$

For a single-layer AR coating, the refractive index of the coating n_1 must satisfy $n_1 = \sqrt{n_0 n_s}$ (where $n_0 \approx 1$ is the refractive index of the air, and n_s is the refractive index of the substrate). In the case of Nd- or Er-doped phosphate glass, $n_1 \approx 1.24$. However, selecting a transparent material with such a low refractive index is nearly impossible, necessitating the use of intermediate

layers such as porous films or nanostructures, which introduce challenges in cost and fabrication processes [12, 13]. As mentioned earlier, to mitigate laser-induced damage to AR coatings, the number of layers in AR coatings is typically increased to form a multilayer system. For a two-layer coating, assuming the layers are homogeneous and their thicknesses satisfy $n_j \cdot d_j = \lambda/4$, the relationship between the refractive indices of the coating layers to achieve $R = 0$ is given by:

$$\frac{n_2}{n_1} = \frac{1}{\sqrt{n_s}} \approx 0.807. \tag{4}$$

In the near-infrared region, several coating materials have been proposed for laser applications, with their refractive indices evaluated at 1053 nm: TiO_2 ($n = 2.31$), Al_2O_3 ($n = 1.64$), HfO_2 ($n = 2.06$), Nb_2O_5 ($n = 2.25$), SiO_2 ($n = 1.47$), and MgF_2 ($n = 1.42$) [8–10]. Eq. (4) represents the ideal condition for a two-layer AR system, in practice this relationship is meaningful only when suitable material pairs exist. For TiO_2–MgF_2, the refractive-index ratio ($n_2/n_1 = 0.615$) differs significantly from the ideal value. Therefore, thickness optimization rather than quarter-wave conditions is required. In this study, TiO_2 and MgF_2 were chosen as the AR-coating materials because they are widely used, cost-effective, and their deposition processes are already well-established on the SYRUSpro 710 system. Although other material pairs such as HfO_2/Al_2O_3 or Al_2O_3/MgF_2 can also be deposited on the same system, they require further process optimization to achieve stable refractive indices and low absorption.

The TiO_2–MgF_2 pair provides substantial index contrast and has been widely recognized as an effective AR-coating combination in optoelectronic and laser applications [20, 21]. TiO_2 was selected as the high-index layer ($n \approx 2.31$ at 1053 nm and $n \approx 2.29$ at 1535 nm [22]) owing to its stable optical properties, strong enough adhesion to phosphate glass, and suitability for electron beam evaporation despite the need for pre-melting [5]. MgF_2, with $n \approx 1.418$ at 1053 nm and $n \approx 1.417$ at 1535 nm [23], was chosen as the low-index layer because it is practical, durable, and offers the lowest available refractive index for thermal evaporation. In the two-layer TiO_2–MgF_2 system, the contrast between high and low indices enables interference cancellation with optimized thickness rather than relying on a single-layer condition. The coating fabrication was performed using the SYRUSpro 710 vacuum system, and the design was fine-tuned with TFCalc to minimize reflectance (see Table 2).

The coating designs were optimized using TFCalc (Software Spectra, Inc.), a professional thin-film design software (latest version 3.6.2). TFCalc simulates multilayer optical coatings with thousands of layers and provides advanced optimization tools such as needle optimization and sensitivity analysis [24, Software Spectra Inc.; HULINKS Co. Ltd.].

2.2. Experimental fabrication and LIDT testing

The TiO_2–MgF_2 anti-reflection coatings were deposited on Nd- and Er-doped phosphate glass substrates using a SYRUSpro 710 vacuum coating system (Bühler Leybold Optics), as shown in Fig. 1. Each coating consisted of two layers (TiO_2/MgF_2) designed to minimize reflectance at 1053 nm for Nd-doped and 1535 nm for Er-doped glass. The deposition was carried out under a base pressure of 5×10^{-6} mbar. The substrates were preheated to 280°C and plasma-cleaned to remove contaminants before coating. TiO_2 (99.99%) was deposited by electron-beam evaporation at a rate of 0.25 nm/s in an oxygen flow of 15 sccm, while MgF_2 (99.99%) was deposited by thermal evaporation at 0.8 nm/s. Additionally, the TiO_2 and MgF_2 layer thicknesses were monitored in real

Table 2. Optical parameters of the optimized TFCalc designs for the two-layer TiO_2-MgF_2 anti-reflection coating on Nd- and Er-doped glass.

	Nd-doped			Er-doped		
Layer Order	Material	Refractive Index	Thickness, nm	Material	Refractive Index	Thickness, nm
Substrate	Nd-doped glass	1.535	-	Er-doped glass	1.530	-
1	TiO_2	2.31	35	TiO_2	2.29	52
2	MgF_2	1.418	240	MgF_2	1.417	350

time using both a quartz crystal monitor (QCM, XMS system, ±1–2 nm accuracy for hundreds-nanometer films) and an optical monitoring system (OMS). After deposition, the samples were cooled to room temperature and characterized for optical and mechanical properties.

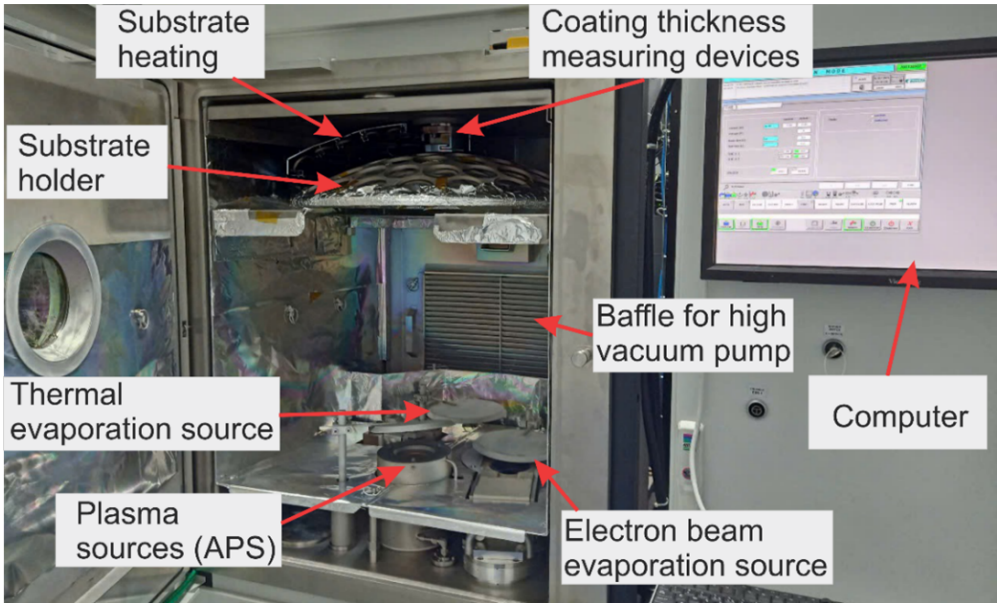

Fig. 1. The SYRUSpro 710 coating system used for depositing the TiO_2-MgF_2 layers.

The transmittance of the AR-coated substrates was measured using a Jasco V-770 UV–Vis–NIR spectrophotometer covering 190–2700 nm, suitable for the target wavelengths of 1053 nm and 1535 nm. Measurements were performed at 25°C with 1 nm spectral resolution and a scan speed of 400 nm/min. Each sample was measured three times for repeatability, and the averaged transmission spectrum was used for analysis. After optical evaluation, the samples underwent durability testing following the MIL-SPEC standards using a testing kit from Edmund Optics [25].

The laser-induced damage threshold (LIDT) defines the maximum laser fluence that an optical coating can withstand before irreversible damage occurs. It is a key parameter indicating the coating's durability under high-power laser irradiation. LIDT testing was performed according to ISO 21254-1:2011 using a nanosecond Nd:YAG laser (LS-2137U-N, LOTIS TII) at 1064 nm, with a pulse width of 10 ns, repetition rate of 10 Hz, and pulse energies from 0.5 to 4 mJ. The laser was linearly polarized (vertical, >100:1) and incident at 5° onto the sample surface through a 300 mm focal-length focusing lens, producing a Gaussian spotwith a $1/e^2$ diameter of $\approx 380\ \mu$m at the sample plane.

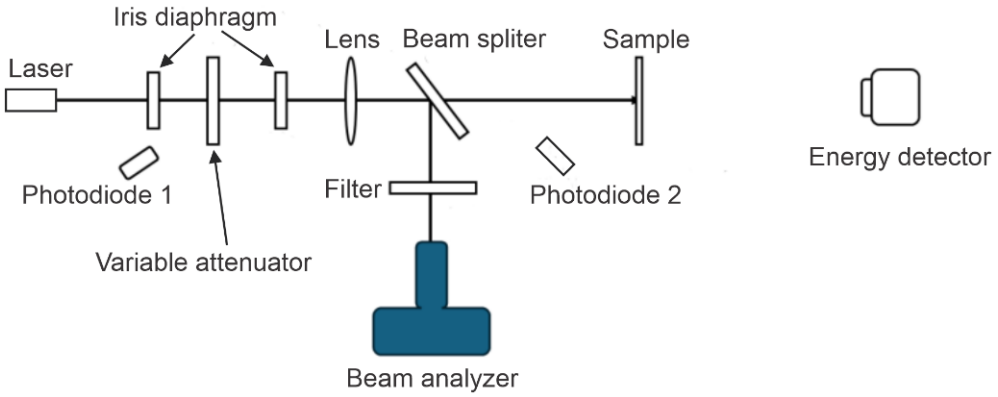

Fig. 2. Experimental setup for laser-induced damage threshold (LIDT) measurement.

The experimental setup, as shown in Fig. 2, included two fast photodiodes (Thorlabs FGA15) for incident and reflected beam monitoring, an energy meter (Coherent) for fluence calibration, a beam analyzer (DataRay WINCAMD UCD) for beam-profile measurement, and a digital oscilloscope (LeCroy 5 GHz) for signal recording.

Tests were carried out under clean laboratory conditions at 25 °C and 60% RH, using both 1-on-1 and 100-on-1 procedures. Damage initiation was identified from sudden spikes in the reflected-signal photodiode and verified by an optical microscope (Nikon). The LIDT value was determined as the lowest fluence causing visible damage, and the damage-probability curve was fitted to obtain the 50% LIDT. In this study, the LIDT measurement was conducted only for the AR-coated sample designed for the Nd-doped glass at 1064 nm, since the available laser source operated at this wavelength.

3. Results and discussion

Figure 3 presents the reflectance spectra of the two-layer TiO_2–MgF_2 anti-reflection coating on Nd- and Er-doped phosphate glass, calculated using the TFCalc-optimized thicknesses. For Nd-doped glass (Fig. 3a), the reflectance reaches a minimum of nearly 0% at 1053 nm, while for Er-doped glass (Fig. 3b), the optimized design achieves a minimum reflectance below 0.1% at 1535 nm. These results confirm that the optimized TiO_2–MgF_2 coating provides excellent anti-reflection performance in the target wavelength ranges.

We present the transmittance spectra of the TiO_2-MgF_2 coating on Nd-doped glass at 1053 nm (a) and Er-doped glass at 1535 nm (b) in Fig. 4, comparing the TFCalc-optimized simulation

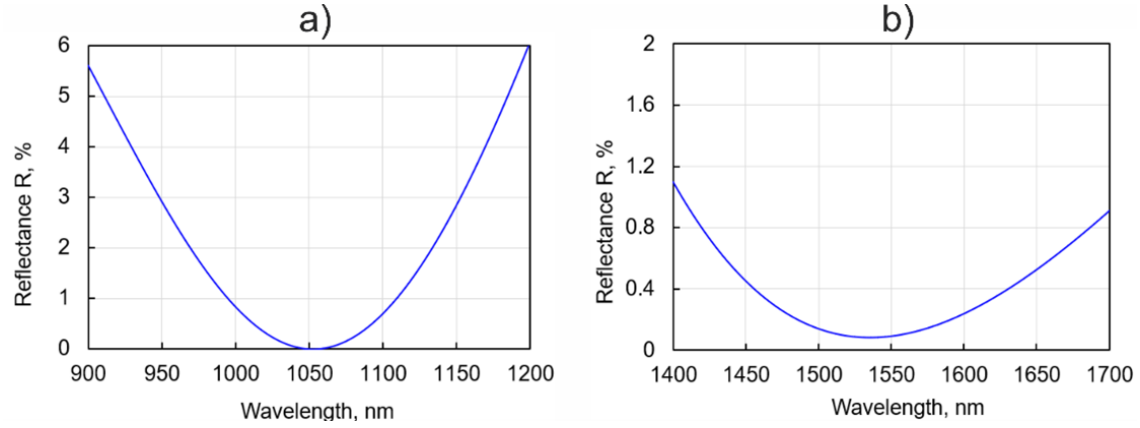

Fig. 3. Reflectance spectra of the TiO_2-MgF_2 coating for the optimized TFCalc designs on Nd-doped glass (a) and Er-doped glass (b).

with experimental measurements conducted on the SYRUSpro 710 system. In Fig. 4a, the simulated transmittance reaches 99.7% at 1053 nm (blue line), while the experimental transmittance exceeds 99.6% across the 1050–1080 nm range (red line). In Fig. 4b, the experimental transmittance achieves 99.8% in the 1530–1570 nm range (red line), corresponding to a reflectance of less than 0.2%, meeting the set target. These results demonstrate that the TiO_2-MgF_2 coating achieves high anti-reflection efficiency, making it suitable for laser optical applications.

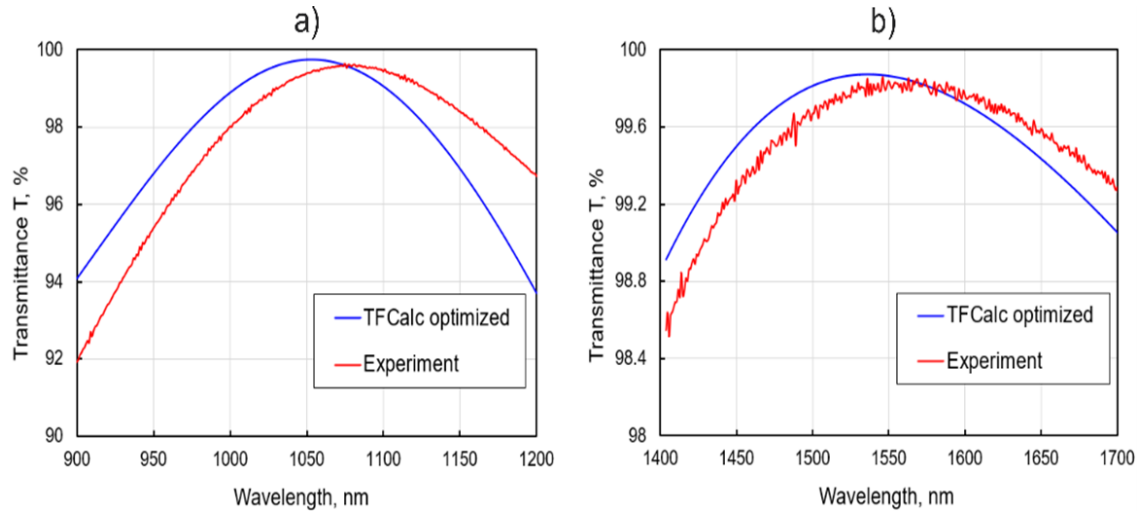

Fig. 4. (Color online) Transmittance spectra of the TiO_2-MgF_2 coating on Nd-doped glass at 1053 nm (a) and Er-doped glass at 1535 nm (b).

Both experimental spectra in Figs. 4(a) and 4(b) show a slight rightward shift compared to the simulations. The dominant cause is most likely the deviation of the actual layer thicknesses from the optimized design, particularly for the very thin TiO_2 layers (35 nm for Nd-doped and

52 nm for Er-doped glass). A secondary contribution may come from slight differences in the refractive indices under deposition conditions, while coating non-uniformity or measurement uncertainty are considered minor effects. Process optimization should therefore focus primarily on improving thickness control.

The durability of the AR coating on Nd- and Er-doped glass substrates was tested using an Edmund Optics kit, following the MIL-C-675, MIL-M-13508, MIL-F-48616, and MIL-PRF-13830B standards [25]. The results confirm that the coating meets the requirements, demonstrating resistance to severe abrasion by passing a test with a 2.5 lb spring-loaded tool over 50 rubbing cycles, as well as moderate abrasion with cheesecloth over 100 cycles. Additionally, the adhesion meets the MIL-M-13508 standard, showing no peeling after a tape test. Combined with the subsequent LIDT evaluation, they indicate that the coating maintains both mechanical and laser-induced robustness, making it well-suited for practical laser applications.

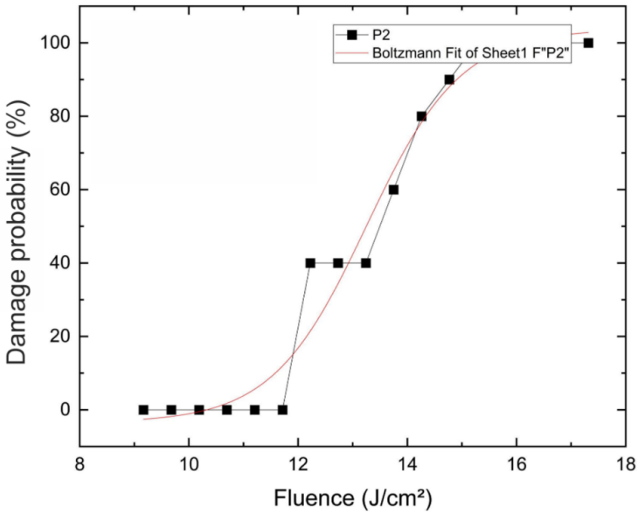

Fig. 5. Laser-induced damage probability curve of the TiO_2–MgF_2 AR-coated Nd-doped glass sample at 1064 nm fitted using a Boltzmann function.

Figure 5 shows the damage-probability curve obtained for the AR-coated Nd-doped glass sample under 1064 nm, 10 ns laser irradiation. The experimental data points were fitted using a Boltzmann sigmoid function, yielding a 50% damage threshold fluence of approximately 13.2 J/cm^2. Minor surface imperfections or microscopic scratches observed on the AR layer may have acted as localized absorption centers, lowering the measured LIDT value.

This threshold value of 13.2 J/cm^2 is considerably higher than the LIDT values reported for TiO_2/SiO_2 multilayer reflective coatings tested under similar laser conditions ($\approx$ 1.5–2.1 J/cm^2 at 1064 nm, 10 ns) [21], but lower than the LIDT of 63 J/cm^2 achieved by the MgF_2 nanoparticle AR coating reported by Chi et al. [26]. The superior performance of the latter mainly stems from the use of a single-layer nanoporous MgF_2 film with high porosity (~50%) [26], which promotes heat dissipation and minimizes optical absorption. The absence of a high-index TiO_2 layer further reduces interfacial electric-field enhancement and thermal stress, both of which typically limit the LIDT of multilayer coatings.

Nevertheless, the achieved value of 13.2 J/cm^2 is sufficient for use in solid-state laser components operating near 1053 nm, especially in applications such as laser rangefinders or medical laser systems where relatively low-fluence pulses are required to avoid optical damage or unwanted thermal effects. For instance, a 1064 nm laser target designator typically delivers pulses of $\geq$ 60 mJ at 1–20 Hz, enabling >10 km ranging [27], while time-of-flight (TOF) rangefinder transmitters based on Q-switched Nd:YAG lasers operate with pulse energies of about 25 mJ, 15 ns pulse duration, achieving measurement ranges of up to 15 km [28].

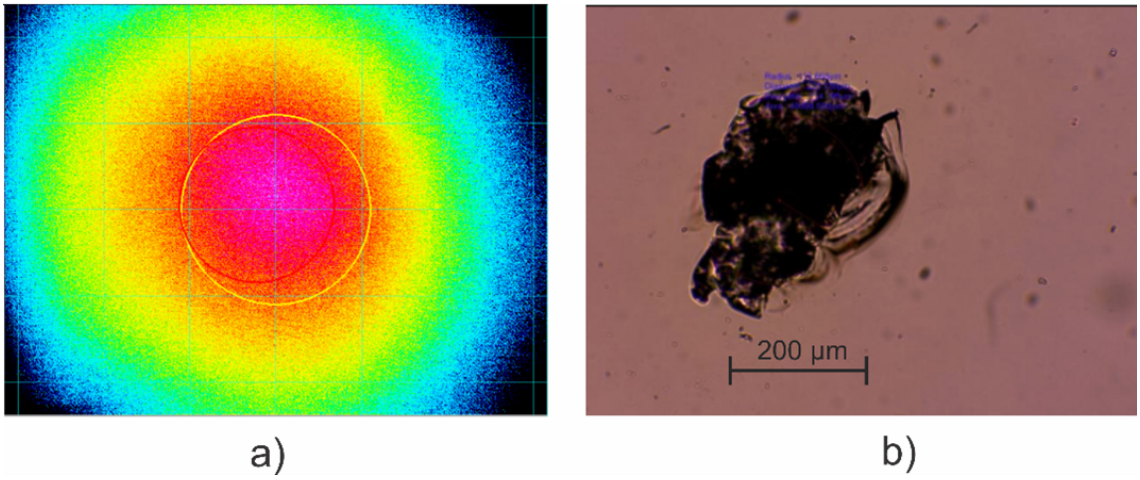

Fig. 6. Beam profile of the incident laser (a) and optical micrograph of the damaged area (b).

Figure 6 presents the beam profile of the incident laser and the optical micrograph of the damaged surface corresponding to the LIDT test. The beam profile and optical micrograph illustrate the Gaussian distribution of the incident laser and the characteristic circular morphology of the damage spot. The pattern observed in the damaged area suggests a typical thermomechanical delamination process occurring at high fluence levels.

4. Conclusion

This work demonstrates the successful fabrication of a two-layer TiO_2–MgF_2 AR coating based on a TFCalc-optimized design, together with a successful LIDT evaluation confirming its applicability in laser systems. Experimental fabrication of the TiO_2-MgF_2 coating on the SYRUS-pro 710 coating system achieved an AR coating reflectance below 0.2%. Transmittance measurements using the Jasco V-770 spectrophotometer yielded values of 99.7% in the 1050–1080 nm range and 99.8% in the 1530–1570 nm range, despite slight discrepancies between the simulations and measurements due to coating thickness variations and fabrication conditions. The coatings also met MIL-SPEC durability standards, confirming high mechanical adhesion and abrasion resistance. In addition, the laser-induced damage threshold test performed on the Nd-doped glass sample at 1064 nm with 10 ns pulses yielded a 50% damage threshold fluence of 13.2 J/cm^2. This value demonstrates that the TiO_2–MgF_2 coating provides reliable laser resistance for solid-state laser components, such as laser rangefinders and low-fluence pulsed medical lasers. Future work will focus on improving thickness control through QCM calibration, stable deposition

rates, and OMS endpoint monitoring, while also exploring alternative material pairs (e.g., Al_2O_3–MgF_2, HfO_2–SiO_2) to benchmark the TiO_2–MgF_2 system and further optimize coatings for high-performance laser applications.

Acknowledgments

The authors sincerely thank Academy of Military Science and Technology for providing the SYRUSpro 710 coating system, Institute of Physics, Vietnam Academy of Science and Technology for supporting the LIDT testing, and Le Quy Don Technical University for providing the coating durability testing kit from Edmund Optics.

Funding

This work was financially supported by the Academy of Military Science and Technology.

Authors contributions

L. V. Dai: Review & editing, Experimentation. D. T. Tung: Methodology, Investigation, Manuscript writing. P. D. Tuan, T. H. Giang: Formal analysis.

Conflict of interest

The authors declare no conflict of interest.

References

[1] S. O. Adeleye, A. A. Adeleke, P. Nzerem, A. I. Olosho, E. N. Anosike-Francis, T. S. Ogedengbe *et al.*, *A review of rare earth ion-doped glasses: Physical, optical, and photoluminescence properties*, Trends Sci. **21** (2024) .

[2] Q. Huang, H. Ding, M. Zhang, S. Bai, S. Dai, Q. Nie *et al.*, *High-Q lasing in Nd^{3+}-doped phosphate glass microsphere resonators*, Opt. Lett. **48** (2023) 3103.

[3] N. G. Boetti, D. Pugliese, E. Ceci-Ginistrelli, J. Lousteau, D. Janner and D. Milanese, *Highly doped phosphate glass fibers for compact lasers and amplifiers: a review*, Appl. Sci. **7** (2017) 1295.

[4] M. Akbulut, L. Kotov, K. Wiersma, J. Zong, M. Li, A. Miller *et al.*, *An eye-safe, sbs-free coherent fiber laser lidar transmitter with millijoule energy and high average power*, Photonics **8** (2021) 8010015.

[5] O. Durante, C. Di Giorgio, V. Granata, J. Neilson, R. Fittipaldi, A. Vecchione *et al.*, *Emergence and evolution of crystallization in TiO_2 thin films: A structural and morphological study*, Nanomaterials **11** (2021) 1409.

[6] M. Akbulut, A. Miller, K. Wiersma, J. Zong, D. Rhonehouse, D. Nguyen *et al.*, *High energy, high average and peak power phosphate-glass fiber amplifiers for 1 micron band*, Fiber Lasers XI: Technol., Syst., Appl. **8961** (2014) 2040721.

[7] J. Zou, H. He, L. Song, L. Huang, J. Lan, L. Lan *et al.*, *Sub-100-fs deep-red mode-locked fiber laser for multicolor two-photon microscopy*, Adv. Photonics **7** (2025) 046009.

[8] Y. Cheng, Q. Yang, Y. Zhu, D. Wu, C. Yu, Y. Sun *et al.*, *Design and fabrication of all-solid anti-resonant silicate fibers for Yb nASE suppression in Er/Yb fiber amplifier*, Opt. Express **32** (2024) 33962.

[9] G. Honciuc, E. Ioffe and J. Kolbe, *Antireflection coatings for high power fiber laser optics*, Photonics Spectra **54** (2020) 44.

[10] T. Tolenis, L. Grinevičiūtė, R. Buzelis, L. Smalakys, E. Pupka, S. Melnikas *et al.*, *Sculptured anti-reflection coatings for high power lasers*, Opt. Mater. Express **7** (2017) 1249.

[11] J. Song, P. Kumar, I. Raouf and H. S. Kim, *Advancements and challenges in anti-reflective coatings: A comprehensive review*, J. Mater. Res. Technol. **39** (2025) 2926.

[12] M. Omrani, M. Malekmohammad and H. Zabolian, *Wide-angle broadband antireflection coatings based on boomerang-like alumina nanostructures in visible region*, Sci. Rep. **12** (2022) 904.

[13] A. H. Jareeze, *Design and simulation antireflection coating for laser nd:yag (1064 nm) wavelength and multifrequency (532, 355 nm) on glass substrate*, Al-Nahrain J. Sci. **11** (2008) 104.
[14] V. H. Mai, C. D. Duong, H. H. Le, L. K. Tran, A. Jaffré, E. Blanc *et al.*, *Simple design of double-layer antireflection coating for Er-doped glass laser application*, Comm. Phys. **32** (2022) 353.
[15] R. Boidin, T. Halenkovič, V. Nazabal, L. Beneš and P. Němec, *Pulsed laser deposited alumina thin films*, Ceram. Int. **42** (2016) 1177.
[16] L. Zhang, L. Hu and S. Jiang, *Progress in Nd^{3+}, Er^{3+}, and Yb^{3+} doped laser glasses at shanghai institute of optics and fine mechanics*, Int. J. Appl. Glass Sci. **9** (2018) 90.
[17] E. Nichelatti, *Complex refractive index of a slab from reflectance and transmittance: analytical solution*, J. Opt. A: Pure Appl. Opt. **4** (2002) 400.
[18] O. Stenzel, *The Physics of Thin Film Optical Spectra*. Springer, Berlin, 2 ed., 2016, 10.1007/978-3-031-65030-7.
[19] G. Rajan, S. Karki, R. W. Collins, N. J. Podraza and S. Marsillac, *Real-time optimization of antireflective coatings for CIGS solar cells*, Materials **13** (2020) 4259.
[20] W. A. Syed, N. Rafiq, A. Ali, R.-u. Din and W. H. Shah, *Multilayer ar coatings of TiO_2/MgF_2 for application in optoelectronic devices*, Optik **136** (2017) 564.
[21] S. Kumar, A. Shankar, N. Kishore, C. Mukherjee, R. Kamparath and S. Thakur, *Laser-induced damage threshold study on TiO_2/SiO_2 multilayer reflective coatings*, Indian J. Phys. **94** (2020) 105.
[22] "Refractive index database of TiO_2." `https://refractiveindex.info`, 2025.
[23] "Refractive index database of MgF_2." `https://refractiveindex.info`, 2025.
[24] "Software for the design and manufacture of optical thin film coatings." HULINKS, `https://www.hulinks.co.jp`, 2025.
[25] "Mil-spec coating testing kit." Edmund Optics, `https://www.edmundoptics.com`, 2025.
[26] F. Chi, G. Wei, Q. Zhang, X. Sun, L. Zhang, X. Lu *et al.*, *Antireflective coatings with adjustable transmittance and high laser-induced damage threshold prepared by deposition of magnesium fluoride nanoparticles*, Appl. Surf. Sci. **356** (2015) 593.
[27] "High-power laser rangefinder and target designator system 60 mj." ERDI-CNLR, `https://www.erdicnlr.com`, 2025.
[28] T. K. Elkhatib and A. M. Mokhtar, *Building and characterization of Q-switched pulsed Nd:YAG laser range finder transmitter*, Int. Conf. Aerosp. Sci. Aviat. Technol. (2017) 1.